Chapter

# Elastic-Based Brittleness Estimation from Seismic Inversion

*Maman Hermana, Deva Prasad Ghosh and Chow Weng Sum*



## Abstract

Information about mechanical rock properties is essential when tight reservoir is to be stimulated using hydrofracturing technique. The brittle area has to be considered as a priority region for determining the location of hydrofracturing initiation. Seismic data are commonly used to estimate the geomechanical properties such as brittleness average from elastic properties: Poisson's ratio and Young's modulus. This paper discusses the process of brittleness estimation based on elastic properties, which can be derived by inverting the pre-stack seismic data that can produce acoustic impedance, shear impedance, and density simultaneously. Novel methods, scaled inverse quality factor of P-wave (SQp) and scaled inverse quality factor of S-wave (SQs) attributes, have been used for identification of brittleness, fracture density, and hydrocarbon bearing in the fractured basement reservoir. The effectiveness of the proposed method has been tested in the field, which is consistent with fracture density log from formation micro-imager (FMI) log and hydrocarbon column data. The result showed that there is a significant correlation between brittleness, estimated from elastic properties, and fracture density logs. New attributes, the SQp attribute is potentially to be used as a fracture density indicator, while SQs attribute indicates the existence of hydrocarbon, which is confirmed with neutron porosity-density logs.

**Keywords:** brittleness average, attribute, crack density, fractured basement, elastic properties



## 1. Introduction

Fractures are important for improving permeability in unconventional reservoirs including shale gas, coal bed methane, tight gas sand, and fractured basement reservoir. In these reservoirs, hydrofracturing is commonly practiced to stimulate fractures and to significantly improve oil/gas flow. The target of hydrofracturing technique is focused on the brittle area (the area with a high tendency to break), which is expected to be able to generate more fractures. To support this objective, understanding of mechanical properties (such as brittleness) of the rock is very important. Estimation of brittleness from seismic data is an important task for better well hydrofracturing and drilling placement.

The success of hydrofracturing depends on the geomechanical brittleness of the formation; brittle rocks tend to generate more fractures compared to ductile rocks. Brittleness is the measurement of stored energy before failure and is a function of

rock strength, lithology, texture, effective stress, temperature, fluid type, digenesis, and TOC [1].

The brittleness is determined by a number of mineral contents of rock. The most brittle minerals like quartz and the less percentage of ductile minerals like clay mineral in the rock tend to make rock more brittle. Rock physics shows that the mineral content determine the elastic properties of rock. Hence, it is reasonable to estimate brittleness using elastic properties. However, the selection of which elastic properties can be used to indicate brittleness is the main task in seismic quantitative interpretation. Estimation of brittleness index which is based on calculation of mineral content and brittleness average which is based on elastic properties and can be derived from seismic data has been successfully applied in the shale gas field [2].

During unconventional reservoir exploration and development, not only how to find out the most brittle area where expected fracture can be generated during horizontal well drilling and hydrofracturing but also how to find the sweet spot where the hydrocarbon is accumulated largely and also how to estimate the capacity and reserve of unconventional reservoir are very challenging. As in case of fractured basement reservoir, the problem on how to find the possible location of generated secondary porosity and permeability and to find where the hydrocarbon accumulation is and what type of hydrocarbon is there is still difficult to be solved and needs advance tool to make more accurate and significant during quantification.

The main objective of this paper is to introduce a new workflow for unconventional reservoir characterization by introducing new attributes: scaled inverse quality factor of P-wave (SQp) and scaled inverse quality factor of S-wave (SQs). These attributes are derived from the attenuation concept through rock physics approximation, which can be implemented on the result of seismic inversion. The existing method, brittleness average, is commonly used to indicate the brittle rock calculated from elastic properties; Poisson's ratio and Young's modulus will be discussed and compared with new attributes to indicate the fracture density. A well data example from fractured basement reservoir in the Malaysian Basin is used to test the performance of these methods to indicate fracture density and hydrocarbon column which also will be discussed.

## 2. Brittleness index (BI) and brittleness average (BA)

Brittleness of rock has been defined in different ways. Jarvie [2] defines the brittleness index (BI) as a fraction of the mineral composition of rock, while Grieser and Bray [3] define brittleness average (BA) as purely related to the elastic properties of the rock.

As mineral composition of rock defines its brittleness, the number of fractions of most brittle mineral impacts on the rock brittleness. Brittleness index (BI) is formulated as

$$BI_{Jarvie} = \frac{Qz}{Qz + Ca + Cly} \tag{1}$$

where $Qz$, $Ca$, and $Cly$ are the fractional quartz content, calcite content, and clay content, respectively.

For wells that are located where the composition of mineral can be properly determined, the BI can be calculated. However, away from the well, the BI is difficult to be estimated due to the difficulties in predicting the mineral content distribution. Hence, it is still difficult to use this technique to estimate brittleness three-dimensionally, because of the challenge in estimating mineral content from seismic data.

Grieser and Bray [3] proposed the use of brittleness average (BA) to express the brittleness of the rock. Brittleness average is calculated based on elastic properties, i.e., normalized Poisson's ratio and Young's modulus. By using this relation, estimation of brittleness in a wider area is possible. Both Young's modulus and Poisson's ratio can be derived from seismic data through seismic inversion. Hence, using this technique the brittleness of rock in terms of BA can be estimated from seismic data.

Young's modulus (E), representing the stiffness of the rock, can be defined in terms of bulk modulus (κ) and Poisson's ratio (σ) as.

$$E = -3\,\kappa\,(1\text{–}2\,\sigma) \tag{2}$$

On the other hand, Poisson's ratio can be derived from P-wave (Vp) and S-wave (Vs) velocities:

$$\sigma = \frac{Vp^2 - Vs^2}{2Vp^2 - 2Vs^2} \tag{3}$$

By substituting Eq. (3) in Eq. (2), the Young modulus is expressed as

$$E = \rho Vs^2 \frac{\left(3Vp^2 - 4Vs^2\right)}{Vp^2 - Vs^2} \tag{4}$$

Hence, the brittleness average (BA) is expressed in Rick's relation [1]:

$$BA = \frac{1}{2}\left(\frac{E - E_{min}}{E_{max} - E_{min}} + \frac{PR - PR_{max}}{PR_{min} - PR_{max}}\right) \times 100 \tag{5}$$

where $E_{min}$ and $E_{max}$ are the minimum and maximum Young's modulus and $PR_{min}$ and $PR_{max}$ are the minimum and maximum Poisson's ratio.

To evaluate the correlation between brittleness average and brittleness geomechanically, the brittleness average is tested against well logs of the domain and compared to geomechanical properties obtained from the formation micro-imager (FMI) log (**Figures 1** and **2**). Examples are taken from a fractured basement reservoir field located in Malaysian offshore. This field is located at a margin of the basin as permo-carboniferous metasediments and volcanic, cretaceous granites, or possibly cretaceous rift fill and mesozoic to carboniferous carbonates and mesozoic granites [4]. The lithology of the offshore basement for this area is described in Tjia et al. [5] based on well drilling distribution with pre-tertiary rock penetration.

**Figure 1** shows the brittleness average logs which is calculated from normalized Poisson's ratio and Young's modulus logs and compared to the core of two different depth samples. The first sample (upper right) was taken from the depth where the brittleness average value is low. In this depth, the core sample showed that only a view number of fractures appear. The crack density of this core sample is low which is correlated with a low value of brittleness average. The second sample (bottom right) was taken from the depth where the brittleness average value is high. Many fractures appeared in this core sample. The core data is taken from a region where the rock is more brittle, which is also associated with a high value of brittleness average in the log. In other words, the intensity of fracture of the rock can be determined by the brittleness average log.

The feasibility study on well log data shows that the brittleness average has a good correlation with fracture density. A high fracture density area is associated

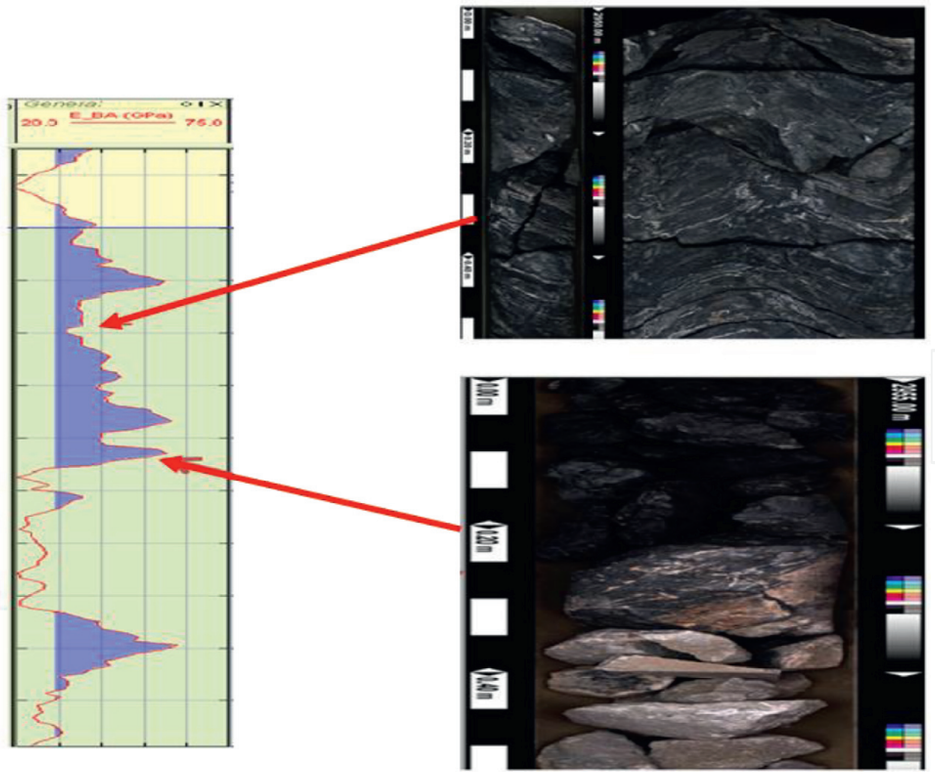


**Figure 1.**
*Brittleness average log (left) compared to the FMI data (right). The high value of brittleness average associated with high crack density.*

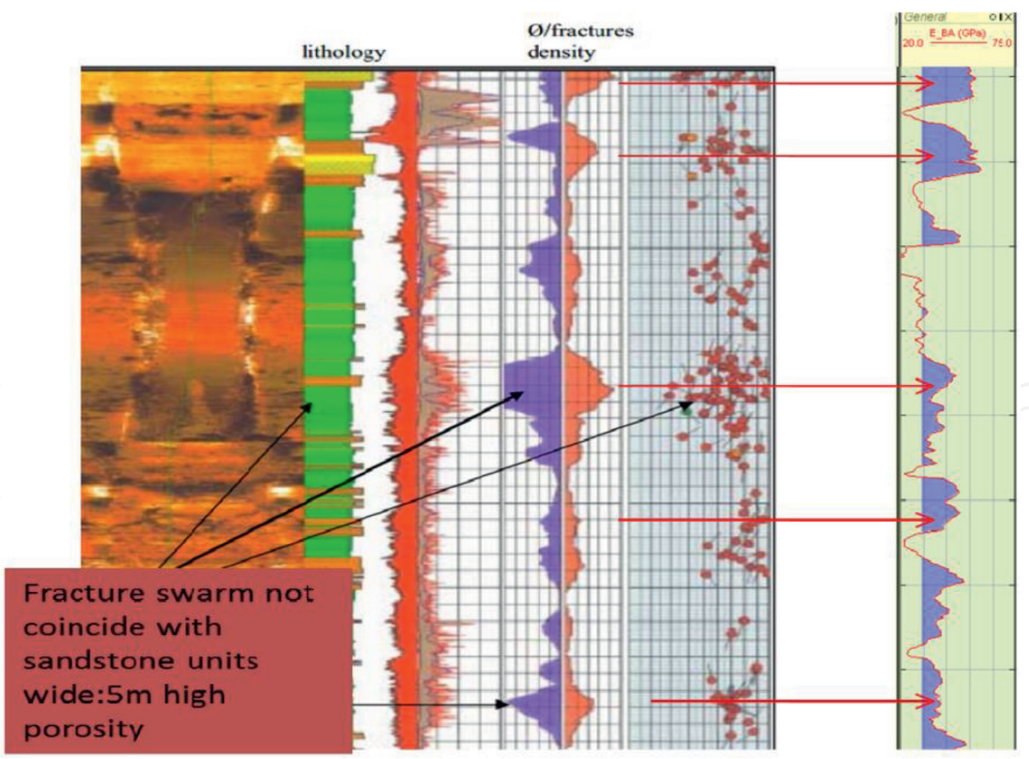


**Figure 2.**
*Lithology and fracture density logs (left) compared with brittleness average (right log).*

with high brittleness average log. Because of the elastic properties, Young's modulus and Poisson's ratio can be extracted from seismic data through inversion result; therefore, the brittleness average, which is associated with fracture density also can be calculated from inversion result.

## 3. SQp and SQs attributes

As in the viscoelastic medium, attenuation and phase velocity of plane wave propagation are governed by the Kramers-Kronig relations [6]. The maximum value of quality factor of P-wave and S-wave which represent the degree of attenuation can be estimated from basic elastic properties of compressional modulus (M) and shear modulus (G) at high- and low-frequency conditions:

$$\begin{aligned} 2Q_p^{-1} &= \frac{M_\infty - M_0}{\sqrt{M_0 M_\infty}} \\ 2Q_s^{-1} &= \frac{G_\infty - G_0}{\sqrt{G_0 G_\infty}} \end{aligned} \tag{6}$$

where the indexes ($\infty$) and ($0$) represent relaxed and unrelaxed conditions, which are still difficult to be measured directly from seismic data.

A high- and low-frequency measurement, in rock physics, can be assumed as an effect of crack by the Hudson crack theory [6]. The changes of anisotropy stiffness component are associated with the difference between compressional modulus at high and low frequencies and can be correlated with Lame parameters: λ and μ. The change in bulk modulus is approximated by

$$\begin{aligned} M_\infty - M_o &= \Delta c_{11}^{Hudson} \\ &\approx \varepsilon \frac{\lambda^2}{\mu} \frac{4(\lambda + 2\mu)}{3(\lambda + \mu)} \end{aligned} \tag{7}$$

And the change in the shear modulus is approximated by

$$\begin{aligned} G_\infty - G_o &= \Delta c_{44}^{Hudson} \\ &\approx \varepsilon \mu \frac{16(\lambda + 2\mu)}{3(3\lambda + 4\mu)} \end{aligned} \tag{8}$$

where ε is the crack density, which is estimated from porosity and aspect ratio (α) as$\varepsilon = 3\phi/(4\pi\alpha)$. By assuming that $M = \sqrt{M_o M_\infty}$ and $G = \sqrt{G_o G_\infty}$, the Qp and Qs are formulated as [6]

$$\begin{aligned} Qp^{-1} &= \frac{2}{3}\varepsilon \frac{(M/G - 2)^2}{(M/G - 1)} \\ Qs^{-1} &= \frac{8}{3}\varepsilon \frac{(M/G)}{(3M/G - 2)} \end{aligned} \tag{9}$$

Information on crack density is indicated by $Qp^{-1}$ and $Qs^{-1}$. If the crack density of the rock increases, the secondary porosity related to the crack will increase, while the bulk density decreases. In other words, an increase in crack density will be followed by a decrease in bulk density. Hence, Eq. (9) can be approximated as [7]

$$\begin{aligned} SQp^{-1} &\equiv \frac{5}{6}\frac{1}{\rho}\frac{(M/G - 2)^2}{(M/G - 1)} \\ SQs^{-1} &\equiv \frac{10}{3}\frac{1}{\rho}\frac{(M/G)}{(3M/G - 2)} \end{aligned} \tag{10}$$

where $SQp^{-1}$ and $SQs^{-1}$ are defined as **scaled inverse Qp** (**SQp**) and **scaled inverse Qs** (**SQs**), which are indicating the attenuation of P and S wave,

respectively. These parameters can be extracted from seismic data through inversion results where M/G is approximated from P- and S-wave velocity ratio or Vp/Vs.

## 4. Approximation of SQp and SQs attributes in the amplitude versus offset (AVO) domain

Derivations of SQp and SQs in the previous sub-chapter show that the parameters are taken from elastic properties extracted from seismic inversion results. To estimate the SQp and SQs directly from seismic data, the approximation of SQp and SQs through the AVO method is proposed.

To understand the approximation of SQp and SQs in the AVO domain, we started with the concept of AVO attributes: AVO intercept and AVO gradient methods. Castagna et al. [8] interprets the AVO intercept and AVO gradient using crossplot method (reader who is interested to get more details on this method can refer to Castagna et al. [8]). In AVO crossplot method, the diagonal line indicates the shale background, and potential hydrocarbon reservoirs will be identified as an AVO anomaly. Determination of the anomaly is measured from the shale background line (**Figure 3**).

The trend or background of Vp/Vs can be approximated with the formula

$$a_b = B/A \tag{11}$$

where B and A are AVO gradient and AVO intercept, respectively. Using Gardner equation [9], the relation between contrast density and contrast velocity is approximated with the formula

$$\frac{\Delta\rho}{\rho} \approx .25\frac{\Delta V_P}{V_P} \tag{12}$$

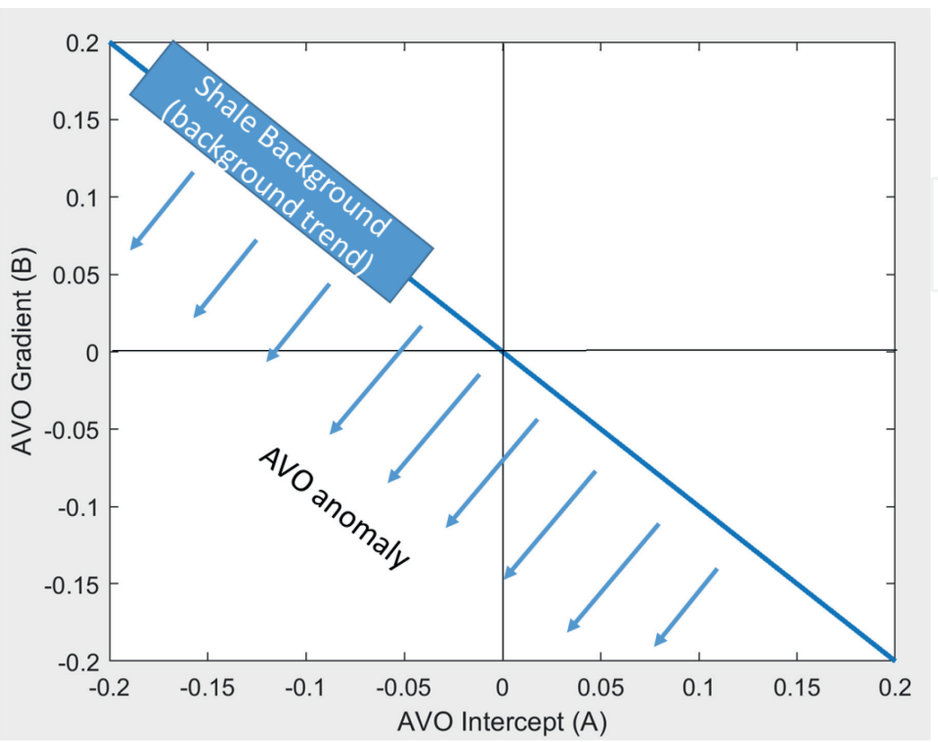


**Figure 3.**
*AVO crossplot method. Diagonal is showing shale background, and hydrocarbon is identified as AVO anomaly.*

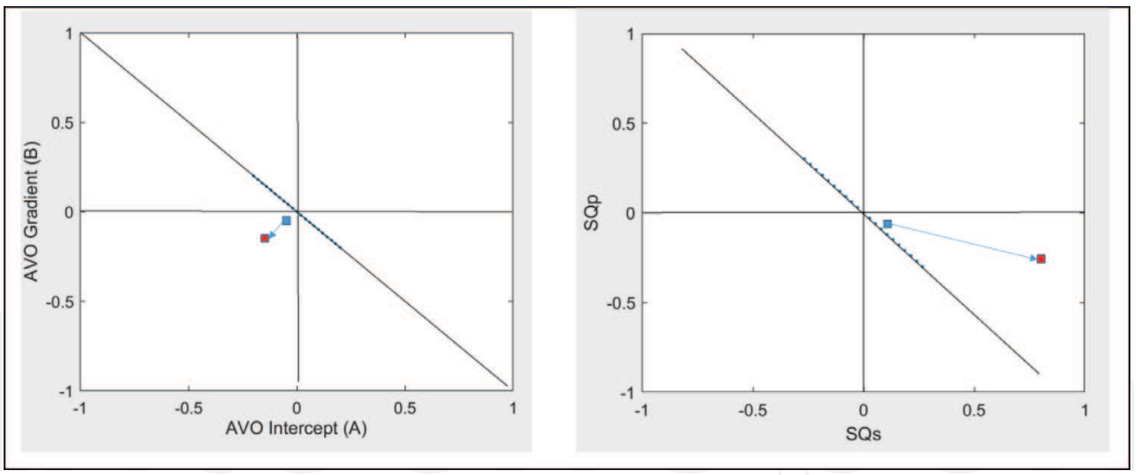


**Figure 4.**
*Comparison between conventional AVO crossplot and new SQp-SQs crossplot.*

where Δ represents the different properties between the upper and lower media. Hence, $\Delta\rho = \rho_2 - \rho_1$, and $\rho = \rho_2 + \rho_1$, $\Delta V_P = V_{P2} - V_{P1}$, and $V_P = V_{P2} + V_{P1}$. The velocity contrast is approximated by

$$\frac{\Delta V_P}{V_P} \approx (8/5)A \tag{13}$$

Combining Eqs. (12) and (13) and substituting Eq. (10), $\mathrm{SQs}^{-1}$ and $\mathrm{SQp}^{-1}$ can be approximated with

$$\begin{aligned} \mathrm{SQp} &\approx \left(\frac{1}{3}\right)A\left(\frac{(-3+2(\mathrm{A}+\mathrm{B}))^2}{2(1-(\mathrm{A}+\mathrm{B}))}\right) \\ \mathrm{SQs} &\approx \left(\frac{4}{3}\right)A\left(\frac{(2(\mathrm{A}+\mathrm{B})-1)}{2(\mathrm{A}+\mathrm{B})+1}\right) \end{aligned} \tag{14}$$

where A and B are the intercept and gradient attributes. Eq. (14) shows that the SQp and SQs attributes can be approximated from the intercept and gradient of AVO.

The crossplot of both methods can be illustrated in **Figure 4**. The potential of hydrocarbon reservoir from oil (blue) to gas (red) is plotted close to each other in the conventional AVO crossplot. However, that anomaly is boosted in the SQp-SQs crossplot. The two different potential reservoirs are separated significantly.

## 5. Numerical testing of SQp and SQs attributes on rock physics model

There are at least two main aspects recorded on seismic data: lithological effect and fluid effect. To understand the effect of both lithological and fluid changes, a rock physics model of soft sediment is used to test the response of SQp and SQs attributes. Initial parameters of model are derived from well log data. Gassmann's fluid substitution was applied on the model to get the new lithology and pore fill at different water saturations and porosities. In this test, the lithological effect is represented by the changes of porosity, while the fluid effect is represented with different water saturation conditions. Water saturation is set from 1 to 100%, where gas is used as a complement, and porosity changes are set from 7 to 25%, while the aspect ratio is assumed to be 0.1. The responses of SQp and SQs attributes at different water saturation and porosity changes are shown in the following figure.

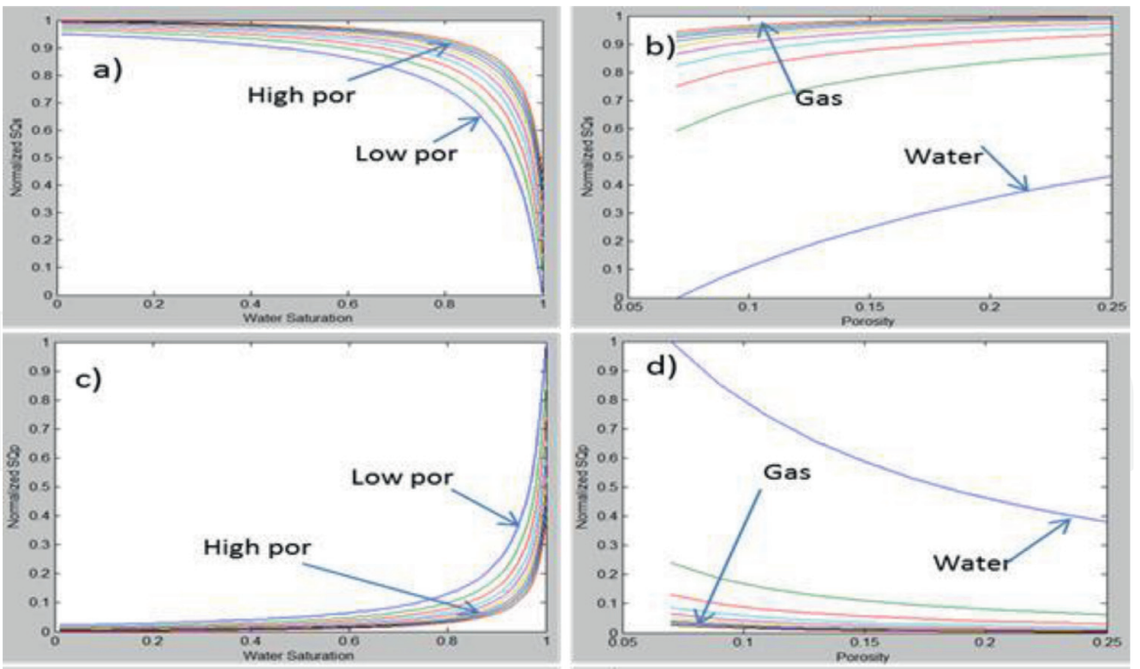


**Figure 5.**
*Responses of SQp and SQs attributes on water saturation changes (left column) and porosity changes (right column). (a) SQs attribute versus water saturation, (b) SQs attribute versus porosity, (c) SQp attribute versus water saturation, and (d) SQp attribute versus porosity. The initial state of the models is Vp = 2231.9 m/s, Vs = 1127.04 m/s, density = 2.11 g/cc, Vsh = 0.56, Sw = 0.49, and porosity = 25%.*

The responses of SQs attribute decrease when water saturation increases (**Figure 5a**). In constant porosity, the SQs value of gas sand is higher than water sand. The porosity changes also affect the SQs attribute; increasing in porosity is followed by increasing in SQs (**Figure 5b**). It can be interpreted also that when porosity of rock increases, the number of fluid inside the rock also increases, which tends to increase the SQs value. This attribute is sensitive to fluid changes (saturation) which means that SQs can be correlated to fluid content conditions. For every different conditions, gas sand has higher SQs value compared to water sand.

**Figure 5c** and **d** shows the SQp responses due to water saturation and porosity changes, respectively. The responses of SQp attribute increase when water saturation increases. However, the increment is significant when the water saturation is close to fully water-saturated conditions. Water saturation is from 0 to about 80%; the increment of SQp is not significant. In the condition where the gas saturation is low (where gas saturation is about 5 or 95% of water), SQp value increases exponentially (**Figure 5c**). This phenomenon is the same as in Gassmann's fluid substitution case where only 5% gas can boost seismic velocity exponentially. On the other side, when porosity increases (where the fluid content is more), the SQp values decrease (**Figure 5d**). It tells us that the number of fluid does not so much affect the SQp. In this example the change of lithology is represented by the change of porosity. SQp is more affected by lithology rather than fluid content. Hence, the SQp attribute might be better as a lithology indicator, while the SQs attribute would be better as a fluid indicator. This hypothesis will be proven by testing the attributes using real data.

## 6. SQp and SQs attribute responses on well domain

Numerical test of SQp and SQs attributes on rock physics shows that the SQp attribute is an indicator of lithological changes, while the SQs attribute can be used

to denote fluid changes. The application of this concept on real well log data can be used to justify this assertion. To do so, another test is carried out to investigate the performance of these attributes in identifying the fluid type and lithological effect. Visual comparison and crossplotting of these attributes on well log data and comparisons with other lithology and fluid indicator (gamma ray and water saturation) logs are presented in **Figure 2**.

**Figure 6a** shows three different reservoir targets, two reservoirs are saturated by gas, and another reservoir is wet (water saturated). All three different reservoirs are indicated as low SQp values. In SQp attribute there is no different responses between gas sand and wet sand; all sand formations are shown as low SQp value. This example shows that SQp attribute is not sensitive with fluid type, only sensitive to the lithology changes. The formation of shale and sand is distinguished clearly as well as in the gamma ray log, while in terms of SQs attribute, both gas and

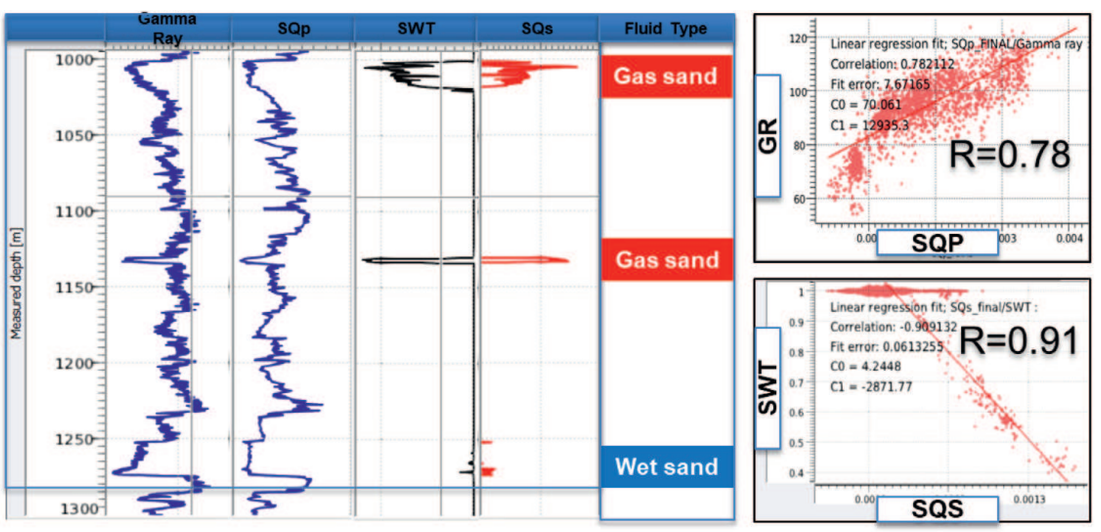


(a)

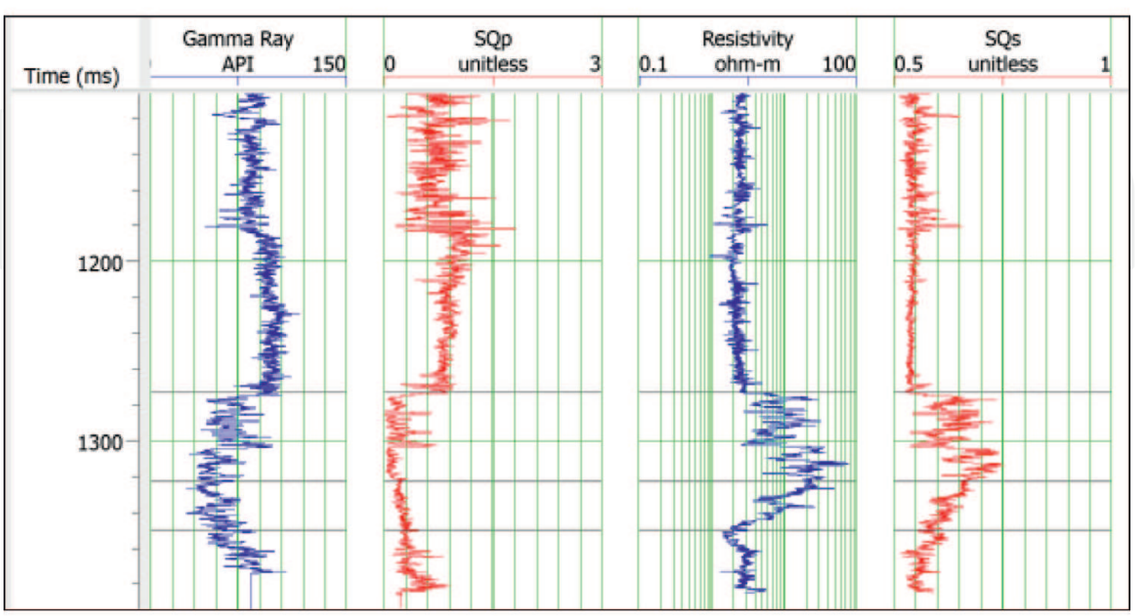


(b)

**Figure 6.**
*(a) SQp and SQs responses compared to lithology log (gamma ray) and water saturation log and its coefficient correlations are obtained from the crossplot (a, right). (b) SQp and SQs test on different well. The SQp attribute is also similar to gamma ray log, and SQs is similar to resistivity logs.*

sand reservoirs have higher value than wet sand. It shows that this attribute is more sensitive to the fluid type than lithology changes. The confirmation of the fluid content is shown by water saturation log, which is also similar to the SQs log.

An example from another field in offshore Malaysia (**Figure 6b**) shows that SQp response is also similar to the gamma ray logs, which supports the hypothesis that this attribute can be used to identify lithology changes in the same way as the gamma ray. Meanwhile, the SQs attribute, which was compared to the resistivity logs, shows that this attribute has high similarity to the resistivity logs. Resistivity log is commonly used to identify the fluid type of the formation; this log is sensitive with the changes of fluid type. Thus, SQs attribute also has potential to be used as fluid indicator. In **Figure 6b**, hydrocarbon formation is indicated by high resistivity value which also is shown in the SQs log. Hydrocarbon formation is indicated as a high SQs value, while brine/water sand will have a lower value.

The separation between lithology and fluid effect is identified easily in the crossplot. Optimum separation between lithological and fluid effects should be orthogonal to each other. To test the effectiveness of SQp and SQs attributes in discriminating the lithology and fluid effect, the crossplot of SQp-SQs has been compared with other elastic properties: lambda-rho vs. mu-rho crossplot as shown in **Figure 7**. The first and second Lame constants (see Section 3) multiplied with density are defined as lambda-rho and mu-rho, respectively. These attributes are a pair of elastic properties that are commonly used to discriminate the lithology and fluid. **Figure 7** shows two different crossplots of mu-rho versus lambda-rho and SQp versus SQs crossplots color-coded by lithology log. All attributes, mu-rho, lambda-rho, SQp, and SQs, are calculated from the same sonic, shear, and density logs. The end members of lithology are classified into four types of lithology: shale sand, wet sand, shaly sand/siltstone sand, and pay sand. The types of lithology are defined by taking the cutoff on the volume of clay, gamma ray, porosity, and water saturation logs. The cutoff for shale was Vclay >0.4, gamma ray >80; shaly siltstone is Vclay <0.4, gamma ray <80, and porosity <0.05; wet sand is Vclay <0.4, porosity >0.05, water saturation >0.85; and pay sand is Vclay <0.4, porosity >0.05, and water saturation <0.85. The lithology log was used to identify the performance or sensitivity of attribute or elastic properties in predicting the lithology and hydrocarbon.

In the mu-rho versus lambda-rho crossplot (**Figure 7a**), gas sand still can be separated from wet sand and shale. However, in this crossplot, it is still difficult to define the separation between lithological and fluid effects. Conversely, in SQp-SQs crossplot (**Figure 7b**), it is not only gas sand and wet sand that are separated, but also the effect of lithology and fluid are separated optimally. In the SQp axis, different lithologies, shale and sand, are distinguished, while in SQs axis that lithology is not separated. The SQs can distinguish gas sand (net pay), wet sand, and shaly sand stone clearly. This SQs axis shows the effect of fluid. Therefore, SQp versus SQs shows an optimum separation between lithological and fluid effect. Lithological effect is distributed along the vertical axis (SQp), while different fluid is distributed along the horizontal axis (SQs). Both lithological and fluid effects are separated orthogonally.

The crossplotting of SQp versus SQs can separate the lithology and pore fluid effects in 90 degrees. It shows that these attributes purely represent either the lithology effect or fluid effect and not both. This orthogonal separation between lithology and pore fluid is the same as what other methods such as the extended elastic impedance (EEI) method would have achieved. In the EEI method, the maximum separation is carried out by projecting the data in the fluid and lithology projection line by calculating the proper chi angle for the projection [10].

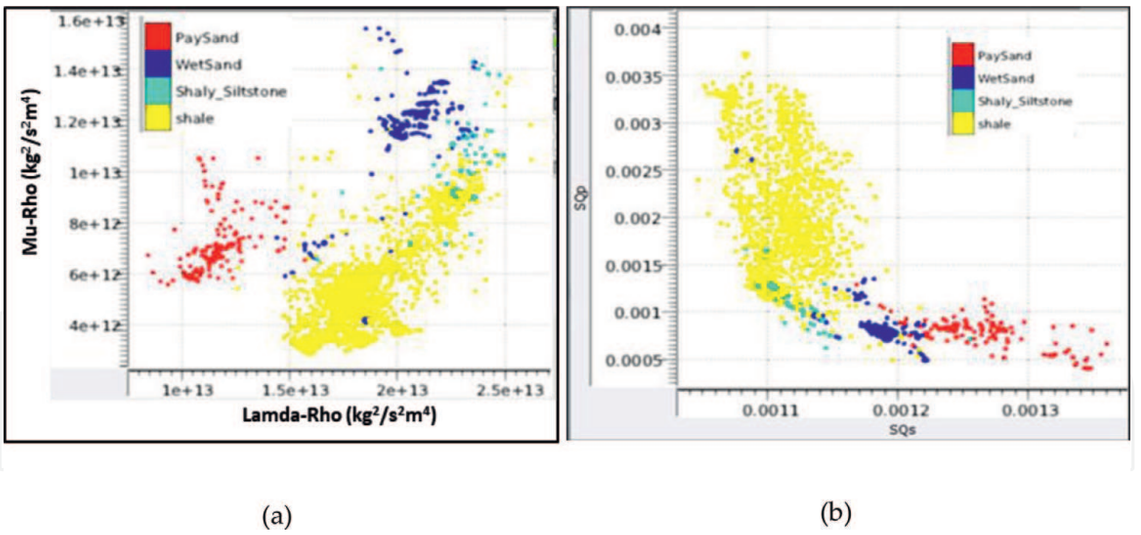


**Figure 7.**
*Lithological and fluid effect separation using crossplot method. (a) Mu-rho versus lambda-rho, (b) SQp versus SQs attribute. The lithology members consist of pay sand (gas sand), wet sand, shaly siltstone, and shale. Data taken from east Malaysian offshore.*

Fortunately, in the SQp and SQp crossplotting, the projection line of lithology and fluid is constructed automatically as the orthogonal axis. This is one advantage when performing the interpretation using this attribute.

## 7. Application of SQp and SQs on fractured basement reservoir case

Previous tests were conducted on conventional reservoirs (clastic reservoir), with the objective being to test the sensitivity of SQp and SQs as indicators of lithology and fluid effect. To test the feasibility of SQp and SQs application on unconventional reservoir characterization, a well log data from fractured basement reservoir was taken from a field in the Malaysian Basin. In this well, the fracture is indicated by the image log. Image log is commonly practiced to detect the fracture of the borehole wall. However, this instrument is sensitive with diameter of borehole size. If there is a bad borehole condition of certain formation, the pad contact of the instrument with the borehole walls is not coupled properly. Hence, the fractures will not be effectively imaged. It is good to have another log as an alternative log that can be associated with the fractures which also can be derived from elastic properties. To fulfill the gap, the SQp and SQs attributes were tested by comparing it with the conventional brittleness average, fracture density log, and neutron porosity-density log to test the effectiveness of new attributes in terms of fracture density and hydrocarbon bearing identification in unconventional reservoir environment.

In this test, sample data was taken from depth 3125 to 3165 m of the fractured basement reservoir formation. The fracture density is compared to the brittleness average logs and SQP and SQS logs (**Figure 8**).

For this formation, the fracture density logs indicate the number of fracture on the formation. Brittleness average logs calculated from Poisson's ratio and Young's modulus was compared with fracture density logs. The results show that the brittleness average is consistent with the number of fracture density as shown in the fracture density logs. In the other side, the SQp log is also similar to the fracture density and brittleness average logs. High value of SQp is related with high fracture density and high brittleness average value. It shows that the SQp attribute also has

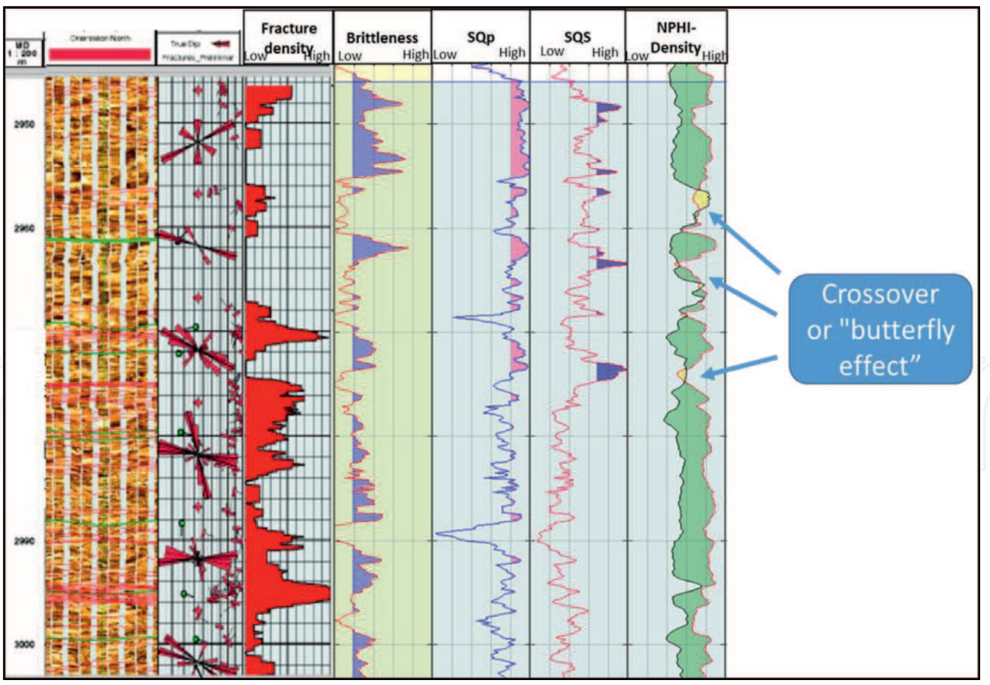


**Figure 8.**
*Comparison between fracture density log, brittleness average log, SQP logs, SQS logs, and density-NPHI logs. Brittleness average looks consistent with fracture density log; SQp attribute is consistent with fracture density and SQs consistent with density-NPHI log.*

potential to be used as a fracture density indicator or brittleness indicator in unconventional reservoir.

The example as shown in **Figure 8** was taken from an oil field-fractured basement reservoir. Conventional interpretation to identified oil column was conducted by interpreting the neutron porosity-density log together. Oil column will be identified as a crossover between neutron porosity and density log. This crossover is called also as "butterfly effect." The crossover of neutron porosity-density logs indicates the oil column. It is clear from **Figure 8** that the "butterfly effect" on neutron porosity-density log is associated with high value of SQs log. As mentioned in the previous test, the high value of SQs is indicating the hydrocarbon location. In this well, the SQs log is consistent with neutron porosity-density logs. It means that if the "butterfly effect" of neutron porosity-density log can be used to indicate hydrocarbon column in the fractured basement reservoir, the SQs attribute also can be used as indicator of hydrocarbon column for this unconventional reservoir environment.

From the test on this fractured basement reservoir well, both brittleness average, which is derived from Poison's ratio and Young's modulus and SQp attribute, have the same chance to be used as fracture density indicators, while the SQs attribute has the same potential as neutron porosity-density log in determining the location of hydrocarbon bearing. The difference is the SQs attribute can be extracted from seismic data, while the neutron porosity-density log can be analyzed on well log only. Hence, the use of SQs attributes can give us advantages to get the hydrocarbon distribution three-dimensionally.

The workflow to obtain the brittleness average and SQp and SQs attributes from seismic data is shown in **Figure 9**. A simultaneous inversion on pre-stack/partial-stack seismic data is needed to obtain P-wave (Vp), S-Wave (Vs), and density, which will be used to calculate the brittleness average and SQp and SQs attributes using Eqs. (5) and (10), respectively. An alternative method of obtaining the SQp and SQs attributes in a reflection domain can be approached using Eq. (14).

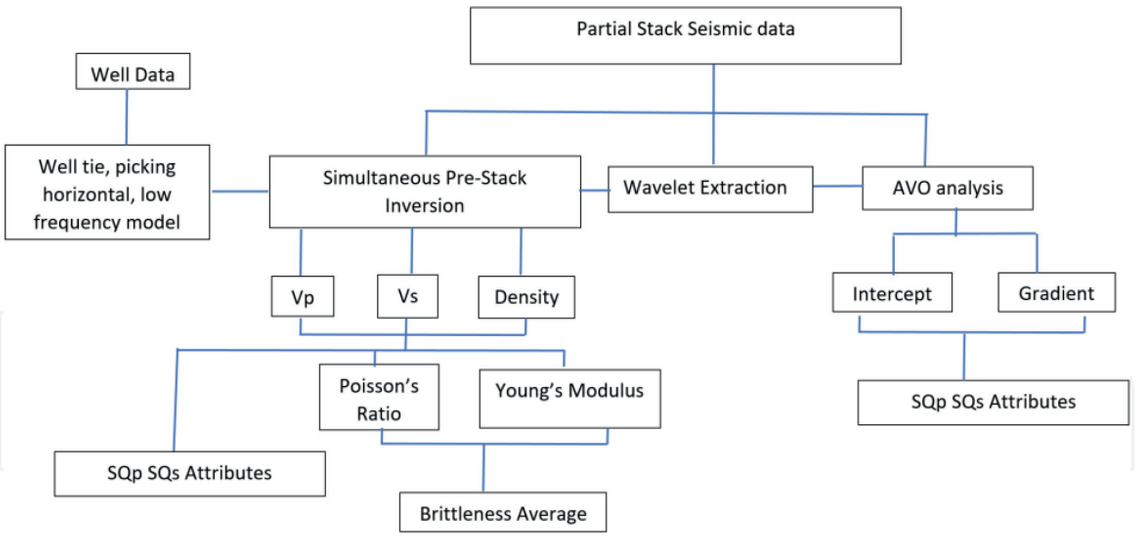


**Figure 9.**
*Workflow for brittleness average and SQp and SQs attribute derivations from seismic data.*

## 8. Conclusions

A common technique for brittleness estimation based on seismic elastic properties has been discussed. The existing method of brittleness average was tested and compared with new attributes (SQp) to indicate the existence of fracture density on a fractured basement reservoir environment in the Malaysian Basin. The results show that SQp attribute coincides with brittleness average and fracture density either on well log data or core data, while the SQs attribute is consistent with neutron porosity-density log which can be used to indicate the hydrocarbon column in the fractured basement reservoir.

Furthermore, the test of SQp and SQs attributes on conventional reservoir shows that those attributes are able to discriminate the lithological and fluid effects optimally. The lithology changes are indicated in the SQp log, which is similar to gamma ray log responses, while the fluid types are distinguished in the SQs log, which is similar to the resistivity log.

One of the advantages of using SQp and SQs attributes for reservoir characterization either in conventional or unconventional reservoir is that the attribute can be not only derived limited on well log domain but also applied three-dimensionally on seismic data. There are two options to get the SQp and SQs from seismic data: based on AVO analysis method and seismic inversion workflow. In the AVO method approach, the anomaly of hydrocarbon reservoir is indicated strongly in the SQp and SQs compared to the conventional AVO analysis using intercept and gradient crossplot method. The application of SQp and SQs attributes through inversion result also gives a strong indicator of lithology and fluid. Due to the similarity of SQp-SQs attributes with petrophysical properties, it is possible to use SQp and SQs attributes for petrophysical property prediction from elastic properties. This will become our future work.

## Acknowledgements

We would like to thank UTP for supporting this research work and PETRONAS for providing the data.

## Author details

Maman Hermana*, Deva Prasad Ghosh and Chow Weng Sum
PETRONAS University of Technology, Seri Iskandar, Malaysia

*Address all correspondence to: maman.hermana@utp.edu.my

## References

[1] Perez R, Marfurt K. Calibration of brittleness to elastic rock properties via mineralogy logs in unconventional reservoirs. In: AAPG International Conference and Exhibition, vol. September; Cartagena, Colombia; 2013

[2] Jarvie DM, Hill RJ, Ruble TE, Pollastro RM. Unconventional shale-gas systems: The Mississippian Barnett shale of north-Central Texas as one model for thermogenic shale-gas assessment. American Association of Petroleum Geologists Bulletin. 2007;**91**(4):475-499

[3] Grieser WV, Bray JM. Identification of production potential in unconventional reservoirs. In: Production and Operations Symposium; 2007

[4] Leo CTAM. Exploration in the Gulf of Thailand in deltaic reservoirs, related to the Bongkot field. Geological Society London Special Publications. 1997; **126**(1):77-87

[5] Tjia AHD et al. In the quest of open fractures in the cystalline basement of the Malay and Penyu Basins. In: Petroleum Geology Conference and Exhibition. 2010; **2010**:124-126

[6] Mavko G, Mukerji T, Dvorkin JP. The Rock Physics Handbook. Calgary, Alberta: Society of Exploration Geophysicists; 2009

[7] Hermana M, Ghosh DP, Sum CW. Discriminating lithology and pore fill in hydrocarbon prediction from seismic elastic inversion using absorption attributes. The Leading Edge. 2017; **36**(11):902-909

[8] Castagna JP, Swan HW, Foster DJ. Framework for AVO gradient and intercept interpretation. Geophysics. 1998;**63**(3):948-956

[9] Gardner GHF, Gardner LW, Gregory R. Formation velocity and density—The diagnostic basics for stratigraphic. Geophysics. 1974;**39**(6):770-780

[10] Whitcombe DN, Connolly PA, Reagan RL, Redshaw TC. Extended elastic impedance for fluid and lithology prediction. In: Mavko G, Mukerji T, Dvorkin J, editors. The Rock Physics Handbook Tools for Seismic Analysis of Porous Media. 2nd edition. Cambridge University Press. 2009;**67**(1):63-67